Cavity-induced chiral edge currents and spontaneous magnetization in two-dimensional electron systems

D. D. Sedov,[1] V. Shirobokov,[1] I. V. Iorsh,[1] and I. V. Tokatly[1,2,3,4]

[1]*ITMO University, Kronverkskiy Prospekt 49, Saint Petersburg 197101, Russia*

[2]*Nano-Bio Spectroscopy Group, Departamento de Polímeros y Materiales Avanzados: Física, Química y Tecnología, European Theoretical Spectroscopy Facility (ETSF), Universidad del País Vasco, Avrnida Tolosa 72, E-20018 San Sebastián, Spain*

[3]*IKERBASQUE, Basque Foundation for Science, 48009 Bilbao, Spain*

[4]*Donostia International Physics Center (DIPC), 20018 Donostia-San Sebastián, Spain*

(Received 15 May 2022; revised 26 October 2022; accepted 31 October 2022; published 9 November 2022)

We consider a laterally confined two-dimensional electron gas (2DEG), placed inside a gyrotropic cavity. Splitting of the circularly polarized electromagnetic modes leads to the emergence of the ground-state spontaneous magnetization, anomalous Hall effect and chiral edge currents in 2DEG. We examine the dependence of the magnetization and edge current density on the system size for two particular cases of the confining potential: infinite wall and parabolic potentials. We show that paramagnetic and diamagnetic contributions to the edge currents have qualitatively different dependences on the system size. For sufficiently large systems the emergent magnetic moment scales with the number of particles and takes a universal value independent of the system shape, the form of confining potential, and the presence of interparticle interactions. These findings pave the route to the design quantum electrodynamic engineering of the material properties of the mesoscopic electron systems.

DOI: 10.1103/PhysRevB.106.205114

I. INTRODUCTION

In recent years, advances in nanofabrication allowed to push the characteristic energies of light-matter interaction in nanosystems embedded in the cavities to the values comparable to cavity photon [1,2] energy. This enabled access to the regime of the so-called ultrastrong coupling between light and matter [3]. One of the main consequences of the onset of ultrastrong coupling is the finite occupation number of the cavity photons even in the ground state of the system. This, in turn, may result in a substantial modification of the material properties when it is embedded in the cavity, which even triggered the emergence of the new field, *Cavity QED materials engineering* [4–6]. The emergent effects include cavity-mediated superconductivity [7–11], ferroelectric phase transitions [12], topological phase transitions [13,14], as well as substantial modification of the chemical reactions inside the cavity [15–21].

For most of the systems, the dipole approximation, assuming that the cavity photon field is spatially homogeneous, holds since the characteristic wavelength of the cavity photon is typically orders of magnitude larger than the characteristic length scale of the material system. At the same time, it has been anticipated that the superradiant phase transitions are forbidden in the cavities with spatially homogeneous modes [22–24], although the debates on the general possibility of such transition are still ongoing [25]. Therefore, it is of great interest to investigate the properties of the electronic system placed inside a gyrotropic cavity which supports nontrivial phenomena even in the dipole approximation as it is presented in this paper.

It has been recently shown that for the macroscopic numbers of two-level systems, the cavity-mediated corrections to macroscopic observables depend only on the effective coupling of a single two-level system to the cavity and, thus, vanish in the thermodynamic limit [26]. Simultaneously, it is well known that for a case of a single two-level system in a cavity, described by the celebrated Rabi model [27], ultrastrong light-matter coupling may lead to the substantial modification of the ground state and even to the quantum phase transitions [28]. Thus, useful results can be obtained by analyzing the dependence of the cavity-mediated corrections to the ground state and various observables on the system size. This utility of such of these results is supported by the fact that most of the current material systems in the cavity QED experiments belong to the mesoscopic class comprising large but finite number of particles.

In this paper, we analyze the cavity-mediated corrections to the ground state and observables for the case of laterally confined two-dimensional electron gas placed in a gyrotropic cavity. We have previously considered this system in the thermodynamic limit [29] and showed that gyrotropy of the cavity leads to the finite Hall conductivity and to the macroscopic magnetization. Here, we derive the explicit dependence of the magnetization on the system size and electronic concentration for the two specific confining potentials: rectangular well and parabolic potential. Moreover, we derive the expressions for the frequency-dependent anomalous Hall conductivity for the case of disordered electron gas and lossy cavity.

The paper is organized as follows. In Sec. II we obtain the general expressions for the diamagnetic and paramagnetic contributions for the case of arbitrary confining potential and

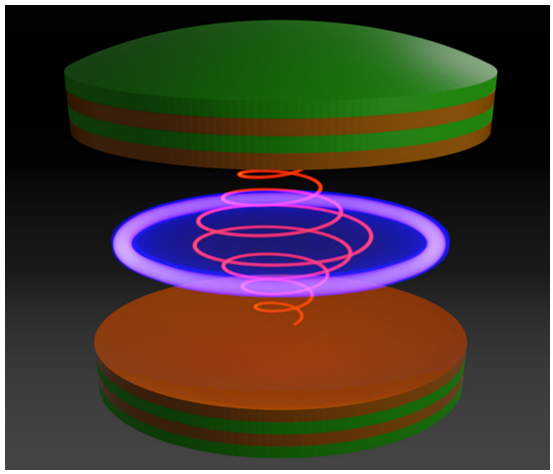

FIG. 1. Geometry of the structure. Two-dimensional electron gas is placed inside a Fabry-Pérot cavity with ferromagnetic mirrors. Magnetization of the mirrors results in the energy splitting between circularly polarized cavity modes, which, in its turn induces the anomalous magnetization of the 2DEG.

apply them to two particular cases of the square well potential (Sec. II A) and the harmonic-oscillator potential. In Sec. III we obtain the expressions for the anomalous Hall conductivity for the case of disordered electron gas in a lossy cavity. In Sec. IV we provide the summary of the results, conclusions, and outlook.

II. EDGE CURRENTS IN THE LATERALLY CONFINED TWO-DIMENSIONAL ELECTRON SYSTEM

Previously [29] we have considered the system schematically depicted in Fig. 1: two-dimensional electron gas (2DEG) placed inside a gyrotropic cavity which is modeled by the vacuum layer sandwitched between two semi-infinite ferromagnetic metals. Even though magnetic materials provide a plethora of different megneto-optical phenomena, for our purposes, the only important thing is that magnetization of the mirrors results in the energy splitting between circularly polarized cavity modes and in time-symmetry breaking which makes it possible to observe spontaneous currents and magnetization of 2DEG as will be shown later. The geometry shown in Fig. 1 comprises two ferromagnetic mirrors inducing the Faraday rotation of the reflected light and as, thus, inducing the splitting of the circularly polarized modes. At the same time, there exist a number of alternative geometries for the chiral and gyrotropic cavities discussed in Ref. [4]. In Ref. [29] we have derived an effective Hamiltonian for the cavity shown in Fig. 1 yielding

$$H_{\mathrm{EM}} = \frac{\Omega_0^2}{2}\mathbf{q}^2 + \frac{1}{2}[\boldsymbol{\pi} + \Delta(\hat{\mathbf{z}} \times \mathbf{q})]^2, \tag{1}$$

where $\mathbf{q}$ and $\boldsymbol{\pi}$ are the canonically conjugated photonic coordinate and the momentum lying on the (xy) plane, $[q_i, \pi_j] = i\delta_{ij}$; Δ is the gyration parameter responsible for lifting degeneracy between left- and right-polarized photon modes. The operator of the cavity vector potential is given as $A_{x,y} \propto q_{x,y}\phi(z)$, where $\phi(z)$ is the normalized mode profile which is omitted further by considering the dipole approximation.

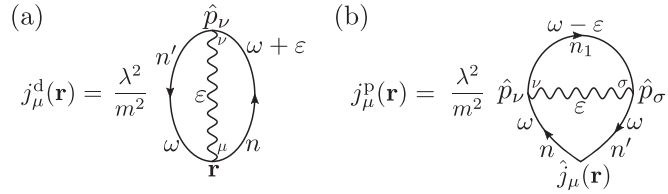

FIG. 2. The diagrammatic representation of (a) diamagnetic and (b) paramagnetic parts of the current. Here solid lines correspond to the electron Green's function $G(\omega, n)$, and wavy lines stand for the cavity EM field propagator $D_{\mu\nu}(\varepsilon)$.

Two eigenmodes of this Hamiltonian correspond to circularly polarized modes with energy splitting between them equals Δ.

The Hamiltonian of 2DEG coupled to the cavity electromagnetic (EM) field via a constant λ reads

$$H_e = \int d^2r\, \psi^*(\mathbf{r})\left[\frac{(\hat{\mathbf{p}} - \lambda\mathbf{q})^2}{2m} + U(\mathbf{r}) - \mu\right]\psi(\mathbf{r}), \tag{2}$$

where $\psi(\mathbf{r})$ is the electron field operator, $\hat{\mathbf{p}} = -i\nabla$, μ is the chemical potential, and $U(\mathbf{r})$ is a confining potential. In general, the Hamiltonian may also include a direct instantaneous Coulomb interaction between electrons. We should stress here that the coupling constant is considered to be independent of the system size so that our analysis is neglecting the dependance of spatially uniform EM field modes on the system size.

We primarily focus on the ground-state current induced by the cavity EM field which is given as follows:

$$j_\mu(\mathbf{r}) = \frac{1}{2m}\langle\psi^*(\mathbf{r})\hat{p}_\mu\psi(\mathbf{r}) - [\hat{p}_\mu\psi^*(\mathbf{r})]\psi(\mathbf{r})\rangle - \frac{\lambda}{m}\langle q_\mu\psi^*(\mathbf{r})\psi(\mathbf{r})\rangle, \tag{3}$$

where the first and the second terms correspond to the paramagnetic and diamagnetic contributions, respectively. Herein, the equilibrium expectation value of an arbitrary operator A is calculated using the Matsubara functional integral approach, $\langle A\rangle = 1/Z\int D[\psi^*, \psi, \mathbf{q}]Ae^S$, $Z = \int D[\psi^*, \psi, \mathbf{q}]e^S$ with an action S describing evolution in the imaginary time from 0 to $\beta = 1/T$. We calculate the perturbative current straightforwardly by expanding the exponent e^S in the powers of λ. The Matsubara functional integral formalism is described in details in Appendix A.

Diagrams corresponding to the lowest-order nonvanishing contributions to the diamagnetic and paramagnetic currents are shown in Fig. 2. Since the diamagnetic current by its origin is proportional to the coupling constant, the simplest term, quadratic to all fields, can be constructed by connecting $\lambda q_\mu\psi^*(\mathbf{r})\psi(\mathbf{r})$ with the interaction $\lambda\mathbf{q}\cdot[\psi^*(\mathbf{r})(\hat{\mathbf{p}}/2m)\psi(\mathbf{r})]$. It evidently results in the diagram describing the diamagnetic part of the current in Fig. 2(a) which is just the product of the photon propagator and the density-current response function,

$$j_\mu^{\mathrm{d}}(\mathbf{r}) = \frac{\lambda^2}{m\beta}\sum_\varepsilon D_{\mu\nu}(\varepsilon)\int d\mathbf{r}'\chi_{n,j_\nu}(\mathbf{r}, \mathbf{r}', \varepsilon), \tag{4}$$

where $D_{\mu\nu}(\varepsilon) = \langle q_\mu(-\varepsilon) q_\nu(\varepsilon)\rangle_0$ is the photon Green's function, corresponding to the photon Hamiltonian (1),

$$[D^{-1}]_{\mu\nu} = \left(\varepsilon^2 + \Omega_0^2\right)\delta_{\mu\nu} - 2\varepsilon\,\Delta\,\epsilon_{z\mu\nu}. \tag{5}$$

Its off-diagonal components, which reflect the gyrotropy of the cavity, explicitly read

$$D_{yx}(\varepsilon) = -D_{xy}(\varepsilon) = \frac{-2\Delta\varepsilon}{(\varepsilon^2+\Omega_+^2)(\varepsilon^2+\Omega_-^2)}, \tag{6}$$

where $\Omega_\pm = \sqrt{\Omega_0^2+\Delta^2} \pm \Delta$ are the frequencies of the left- and right-polarized modes. Correlator $\chi_{n,j_\nu}(\mathbf{r},\mathbf{r}',\varepsilon) = \langle n(\mathbf{r},\varepsilon) j_\nu(\mathbf{r}',-\varepsilon)\rangle_0$ is the density-current Matsubara response function in the system without electron-photon coupling.

By expanding e^S up to the second order of λ and averaging the expression for the paramagnetic current with two interactions $\lambda\mathbf{q}\cdot[\psi^*(\mathbf{r})(\hat{\mathbf{p}}/2m)\psi(\mathbf{r})]$, the nontrivial diagram in Fig. 2(a) can be constructed, thus, we can similarly express paramagnetic current as

$$j_\mu^{\mathrm{p}}(\mathbf{r}) = \frac{\lambda^2}{\beta}\sum_\varepsilon D_{\nu\sigma}(\varepsilon)\int d\mathbf{r}' d\mathbf{r}'' \chi_{j_\mu,j_\nu,j_\sigma}(\mathbf{r},\mathbf{r}',\mathbf{r}'',\varepsilon), \tag{7}$$

where $\chi_{j_\mu,j_\nu,j_\sigma}(\mathbf{r},\mathbf{r}',\mathbf{r}'',\varepsilon) = \langle j_\mu(\mathbf{r}) j_\nu(\mathbf{r}',\varepsilon) j_\sigma(\mathbf{r}'',-\varepsilon)\rangle_0$ is the nonlinear current response function. The appearance of nonlinearity here can be understood physically: The current is created by the fluctuations of the electric-field $\langle E^2\rangle$ interacting with electrons, not by the electric field itself which is equal to zero. Apparently the above general expressions for the currents in terms of response functions are also valid for the interacting electron gas. Diagrammatically, inclusion of the Coulomb interaction corresponds to "decorating" graphs in Fig. 2 by all possible insertions of the interaction lines, which produces the exact response functions. It is also worth noting that the sum of the two contributions, Eqs. (4) and (7), relates the equilibrium current in a quantum cavity with a gyrotropic vacuum to a response function describing a classical photogalvanic effect.

As we show in Appendix C, in the case of a system confined by a potential that is translation invariant in one direction, the paramagnetic contribution of Eq. (7) vanishes identically. We, therefore, expect that this part of the current will be negligible for any sufficiently large system with smooth edges.

For some special simple geometries, for example for a semi-infinite sample bounded by a flat edge, the diamagnetic contribution to the current density can be calculated exactly. This can be performed using the following sum rule (so-called acceleration identity) for the density-current response function [30]:

$$\int d\mathbf{r}'\chi_{n,j_\nu}(\mathbf{r},\mathbf{r}',\varepsilon) = \frac{1}{m\varepsilon}\left[-\nabla_{r_\nu} n(\mathbf{r}) + \int d\mathbf{r}'\chi_{n,n}(\mathbf{r},\mathbf{r}',\varepsilon)\nabla_{r'_\nu} U(\mathbf{r}')\right], \tag{8}$$

where $n(\mathbf{r})$ is the electron density, $\chi_{n,n}(\varepsilon)$ is the density response function, and U is the external potential which may include both the confining potential and possibly a disorder potential. Let us consider a confining potential corresponding to a single edge along the y direction, which separates the regions of zero density well outside the sample, and a finite density $n(\mathbf{r}) = n_0$ deeply inside. The total current along the edge is calculated by integrating the current density of Eq. (4), $J_y \sim \int d\mathbf{r} j_y^d(\mathbf{r})$ and using the identity Eq. (8) for the density-current response function. We can immediately notice that the second term in Eq. (8) vanishes upon integration because the gauge invariance requires $\int d\mathbf{r}\chi_{n,n}(\mathbf{r},\mathbf{r}',\varepsilon) = 0$. The integral of the first term by partial integration reduces to the difference of the densities across the edge and, thus, equals $n_0/m\varepsilon$. As for the translation invariant boundary the paramagnetic current of Eq. (7) vanishes the total edge current can then be expressed as

$$J^y_{\mathrm{edge}} = \frac{\lambda^2 n_0}{m^2\beta}\sum_\varepsilon \frac{D_{yx}(\varepsilon)}{\varepsilon}. \tag{9}$$

We note that this result is universal and holds also for interacting electronic systems. The universal result Eq. (9) is expected to give the edge current of any sufficiently large system. Therefore, it should determine the emergent magnetic moment $\mathbf{m} = \frac{1}{2}\int(\mathbf{r}\times\mathbf{j})d\mathbf{r}$ of a large sample as

$$m_z = -SJ^y_{\mathrm{edge}} = \frac{\lambda^2 N}{m^2\beta}\sum_\varepsilon \frac{D_{yx}(\varepsilon)}{\varepsilon}, \tag{10}$$

where S is the sample area and N is the total number of particles. Below, we study the distribution of the equilibrium current and the magnetization for systems of different sizes and confirm that the above universal results are indeed approached asymptotically.

To explicitly analyze the current density in finite systems, we neglect the electron-electron interaction and compute the current given by two diagrams in Fig. 2. The diamagnetic and paramagnetic contributions can be written as spectral decomposition,

$$j_\mu^d(\mathbf{r}) = \frac{\lambda^2}{m^2\beta^2}\sum_{\omega,\varepsilon}\sum_{n,n'} D_{\mu\nu}(\varepsilon) G(\omega+\varepsilon,n) G(\omega,n') \times p_\nu^{nn'}\psi_{n'}^*(\mathbf{r})\psi_n(\mathbf{r}), \tag{11}$$

$$j_\mu^{\mathrm{p}}(\mathbf{r}) = \frac{\lambda^2}{m^2\beta^2}\sum_{\omega,\varepsilon}\sum_{n,n',n_1} D_{\nu\sigma}(\varepsilon) G(\omega,n) G(\omega,n') \times G(\omega-\varepsilon,n_1) p_\nu^{nn_1} p_\sigma^{n_1 n'} j_\mu^{n'n}(\mathbf{r}), \tag{12}$$

where ω,ε are fermionic and bosonic Matsubara frequencies; index n numerates states of the unperturbed electron system, $G(\omega,n) = -\langle a_n(\omega) a_n^*(\omega)\rangle_0$ is an electron Green's function of the uncoupled system, where $a_n(\omega)$ is an annihilation operator corresponding to the one-particle state $|n\rangle$; $\psi_n(\mathbf{r}) = \langle\mathbf{r}|n\rangle$; $p_\nu^{nn'} = \langle n|\hat{p}|n'\rangle$, $j_\mu^{nn'}(\mathbf{r}) = 1/(2m)[\psi_{n'}^*(\mathbf{r})\hat{p}_\mu\psi_n(\mathbf{r}) - (\hat{p}_\mu\psi_{n'}^*(\mathbf{r}))\psi_n(\mathbf{r})]$.

Summation over fermionic Matsubara frequencies can be performed explicitly, the corresponding result is presented in Appendix B. It is worth mentioning that for bounded systems where eigenfunctions can always be chosen as purely real, the diagonal part of the photonic propagator does not contribute to the current, and only nondiagonal elements induced by the system's gyrotropy result in the nontrivial term.

We now closely examine two particular cases of confining potentials: square well and parabolic potentials.

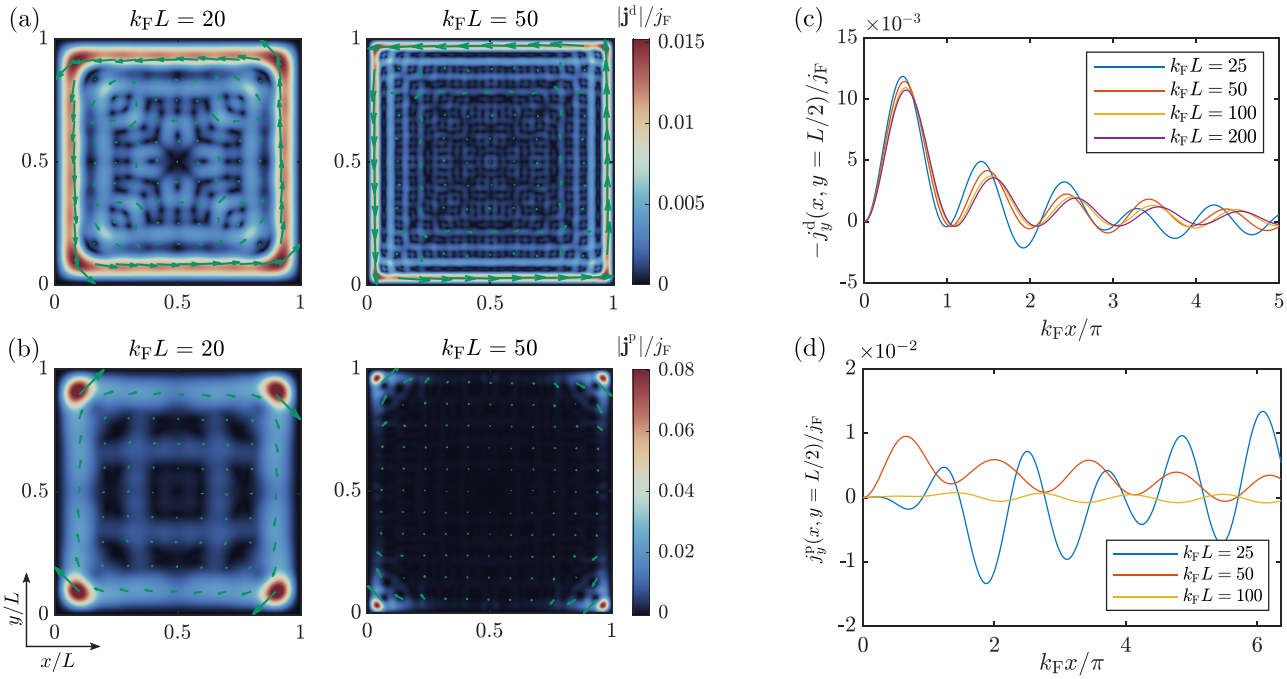

FIG. 3. (a) Spatial distribution of the absolute value of diamagnetic current in the infinite square-well potential for different size parameters k_FL. Green arrows show the direction of current density at a given point. (b) Analogous distribution calculated for the paramagnetic current. (c) and (d) present the y component of diamagnetic and paramagnetic contributions to the current, respectively, taken at $y = L/2$ vs k_Fx. Each dependence is calculated for the following parameters: $\Omega_0/\mu = 1$, $\Delta/\mu = 0.01$, $kT/\mu = 0.01$.

A. Square-well potential

First, we apply the described approach to the case when 2DEG is placed inside a square infinite quantum well with size $L \times L$. An intuitive size parameter for such a system is k_FL, where k_F is the Fermi wave vector. For large k_FL, we expect that effects of the corners to the integral properties and even to the current density almost everywhere can be neglected, the same stands for the the interference between the different edges of the structure. Thus, the general properties in the thermodynamic limit ($k_FL \to \infty$, k_F is fixed) can be understood by considering semi-infinite 2DEG which occupies half-plane $x > 0$. In Appendix C, we present the derivation of both currents. Whereas paramagnetic density is appeared to be locally zero, diamagnetic current is the nontrivial one localized near $x = 0$, and it creates the following edge current obtained by the integration over x,

$$J_{\text{edge}}^{\text{wall}} = -\frac{\lambda^2 n_0 \Delta}{2\Omega_0^2 \tilde{\Omega}_0 m^2}\left[1 + n_{\text{B}}^{+} + \frac{\tilde{\Omega}_0}{\Delta} n_{\text{B}}^{-}\right], \qquad (13)$$

where $\tilde{\Omega}_0 = \sqrt{\Omega_0^2 + \Delta^2}$, $n_{\text{B}}^{\pm} = n_{\text{B}}(\Omega_-) \pm n_{\text{B}}(\Omega_+)$, $\Omega_\pm = \tilde{\Omega}_0 \pm \Delta$, n_0 is the density of electrons in the system, and n_{B} is the Bose-Einstein distribution. We note that this result is very similar to the one obtained for the case of the edge DC current in the 2DEG under classical circularly polarized optical pump in the case of weak disorder potential [31]. In Figs. 3(a) and 3(b) we present spatial distribution of the absolute values of both currents, their vector plots are depicted with green arrows. We normalize our results on $j_F = n_0 v_F (\Delta/\mu)(\lambda^2/m\mu^2)$, where $v_F = \sqrt{2\mu/m}$—electron's speed on the Fermi surface. Numerical calculations show that currents have significantly different bahaviors. Diamagnetic current relatively far away from corners tends to some distribution which can be clearly see in Fig. 3(c), whereas paramagnetic current density has nonzero distribution only near corners.

We also present the convergence of the edge current and magnetization of the system to $J_{\text{edge}}^{\text{wall}}$ with respect to k_FL in Fig. 4. It proves our considerations that in the thermodynamic limit the system is mainly defined by the properties of semi-infinite 2DEG.

B. Harmonic oscillator

Let us consider parabolic confining potential $U(\mathbf{r}) = m\omega^2\mathbf{r}^2/2$—another relatively simple system which allows to

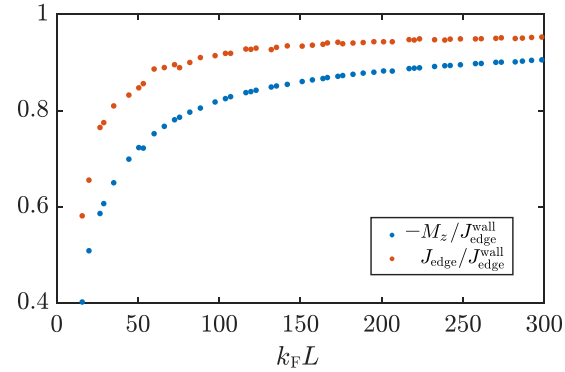

FIG. 4. Convergence of edge current and diamagnetic magnetization of the electron system in the infinite well confining potential to the edge current in the semi-infinite system. At each plotted point, chemical potential μ and density $n = N/S$ are fixed. The following parameters are used: $\Omega_0/\mu = 1$, $\Delta/\mu = 0.01$, $T/\mu = 0.01$.

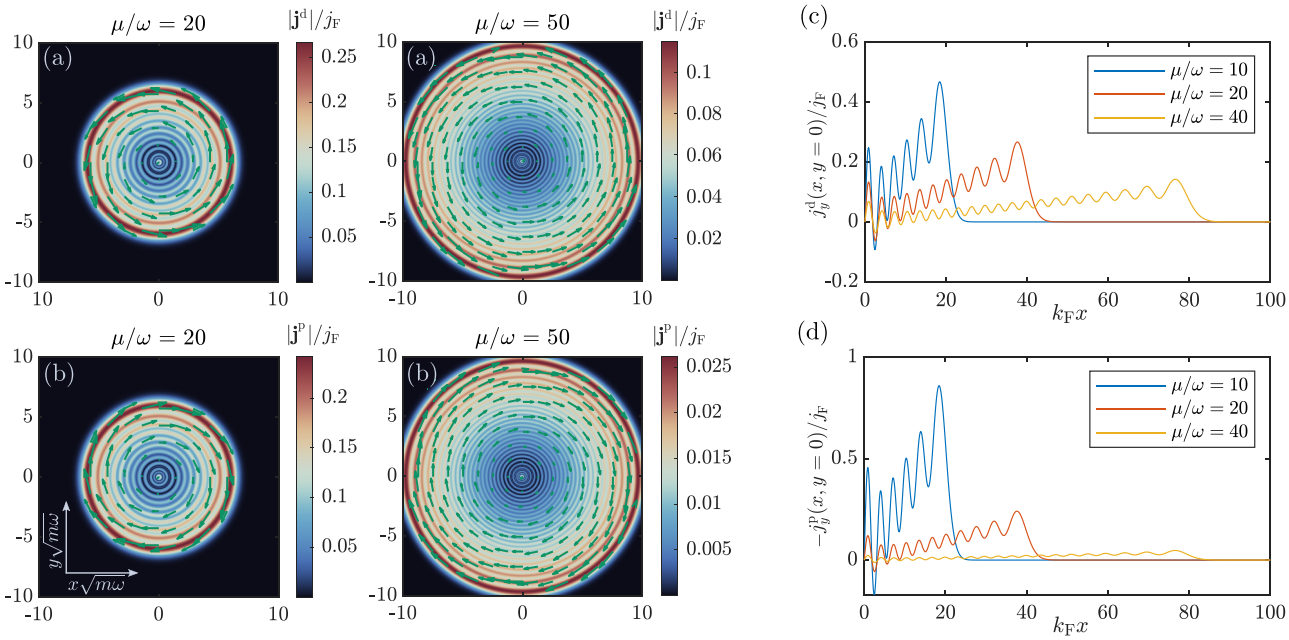

FIG. 5. (a) Spatial distribution of the diamagnetic part of the current in the parabolic potential for two values of μ/ω. (b) Analogous distribution calculated for the paramagnetic current. (c) and (d) present radial distribution of the diamagnetic and paramagnetic contributions to the current, respectively. Each dependence is calculated for the following parameters: $\Omega_0/\mu = 1$, $\Delta/\mu = 0.01$, $kT/\mu = 0.01$.

obtain some analytical results not even in the thermodynamic limit,

$$j_y^d(\mathbf{r}) = \frac{4\lambda^2}{m^2\beta}\sqrt{\frac{m\omega}{2}}\sum_n [f_{n+1} - f_n]\sqrt{n_x+1}\psi_{n_x+1}(x) \times \psi_{n_x}(x)|\psi_{n_y}(y)|^2 \sum_\varepsilon \frac{\varepsilon D_{yx}(\varepsilon)}{\varepsilon^2+\omega^2}, \tag{14}$$

$$j_y^p(\mathbf{r}) = \frac{4\lambda^2\omega^2}{m\beta}\sum_n \psi_{n_x+1}(x)\psi_{n_x}(x)\mathrm{Im}\left[j_y^{n_y+1,n_y}(y)\right] \times \sqrt{(n_x+1)(n_y+1)}[f_{n+2} - 2f_{n+1} + f_n] \times \sum_\varepsilon \frac{\varepsilon D_{yx}(\varepsilon)}{(\varepsilon^2+\omega^2)^2}, \tag{15}$$

where $\psi_{n_x}(x)$ are eigenfunctions of one-dimensional harmonic oscillator, $f_n = f(\omega n)$ is Fermi-Dirac distribution. From the obtained expression one clearly sees that in the low-temperature limit, $T/\mu \to 0$, currents are determined only by the electrons on the Fermi surface.

We present the distributions of currents in Fig. 5. For both contributions, the radius of localization, where currents are not exponentially suppressed, grows as $O(1/\omega)$. It can be understood from the quasiclassical approach in which this radius is given by $\sqrt{2\mu/(m\omega^2)}$. In the low-temperature limit $T/\mu \to 0$, the summation of the eigenstates can be performed yielding the expression for magnetization,

$$m_z^d = \left(\left\lfloor\frac{\mu}{\omega}\right\rfloor^2 + \left\lfloor\frac{\mu}{\omega}\right\rfloor\right)\frac{\lambda^2}{2m^2\beta}\sum_\varepsilon \frac{\varepsilon D_{yx}(\varepsilon)}{\varepsilon^2+\omega^2}, \tag{16}$$

$$m_z^p = -\omega^2\left(\left\lfloor\frac{\mu}{\omega}\right\rfloor^2 + 5\left\lfloor\frac{\mu}{\omega}\right\rfloor + 6\right)\frac{\lambda^2}{3m^2\beta}\sum_\varepsilon \frac{D_{yx}(\varepsilon)}{(\varepsilon^2+\omega^2)^2}, \tag{17}$$

where $\lfloor\cdot\rfloor$ corresponds to the floor function. We also note that the prefactor in Eq. (16) is exactly the doubled number electrons in the system. Interestingly, this result for the diamagnetic magnetization can be also obtained using the identity (8) for arbitrary temperature—this is explained explicitly in Appendix D. The summation over the Matsubara frequencies can also be taken analytically, and the results are presented in Appendix E.

These expressions hold for an arbitrary relation μ/ω and require only low temperatures relative to the chemical potential. Since the number of occupied states in the system is equal to $1/2\lfloor\mu/\omega\rfloor(\lfloor\mu/\omega\rfloor+1)$, we obtain nonzero magnetization in the limit of vanishing oscillator frequency, $\omega/\mu \to 0$, only for the diamagnetic contribution. It coincides with the results we have found for the infinite well potential. It is interesting that the system with completely different potentials inherits this behavior.

It is worth mentioning that our analysis is neglecting the dependence of the coupling constant λ on the size of the cavity mode; for the physical systems, this constant behaves as $O(1/\sqrt{V})$, where V is the mode size. More specifically, it means that the cavity should be much larger than the maximum size of the electron system in the considered series approaching the thermodynamic limit so that the dipole approximation is valid for every characteristic size L. Additional scaling of the cavity size will suppress the observable magnetization.

III. VACUUM ANOMALOUS HALL EFFECT IN THE PRESENCE OF DISORDER AND CAVITY LOSSES

In this section we derive the Hall conductivity of the system from the equations of motions for the observables taking into account disorder in electron gas and cavity losses. First of

all, we note the total field $\mathbf{E}$ comprises the external field $\mathbf{E}_0$ and the cavity field $\mathbf{E}_{\text{cav}}$. The current is connected to the total electric field via the Drude formula $\mathbf{j} = \sigma_D \mathbf{E}$, where $\sigma_D = (ne^2/m)(1 - i\omega\tau)^{-1}$, and τ is the momentum relaxation time. To find the cavity field we note that it is directly related to the time derivative of the average cavity photon coordinate $\mathbf{E}_{\text{cav}} = \lambda\langle\dot{\mathbf{q}}\rangle/e$ which can be extracted from the equation of motion for the photon coordinate derived from the Hamiltonians (1) and (2),

$$\langle\ddot{\mathbf{q}}\rangle - 2\,\Delta\hat{z} \times \langle\dot{\mathbf{q}}\rangle + \Omega_0^2\langle\mathbf{q}\rangle + \gamma\langle\dot{\mathbf{q}}\rangle = \lambda\mathbf{j}, \tag{18}$$

where $\mathbf{v} = \mathbf{j}/(e)$ and γ is the cavity losses rate. We assume that cavity losses very weakly depend on frequency. Since the equation is linear, we can take the Fourier transform and arrive at a linear system of equations. From Eq. (18) we find the expression for the cavity field,

$$\mathbf{E}_{\text{cav}} = -i\omega\lambda^2/(e^2)\hat{D}\mathbf{j}, \tag{19}$$

where $\hat{D}$ is the cavity photon propagator, $[\hat{D}^{-1}]_{xx} = [\hat{D}^{-1}]_{yy} = \Omega_0^2 - \omega(\omega + i\gamma)$ and $[\hat{D}^{-1}]_{xy} = -[\hat{D}^{-1}]_{yx} = -2i\omega\Delta$. The expression for the current then reads

$$\mathbf{j} = \left[\hat{I} + \frac{\omega\tau}{i + \omega\tau}\frac{\lambda^2}{m}\hat{D}\right]^{-1}\sigma_D\mathbf{E}_0, \tag{20}$$

where $\hat{I}$ is the unity matrix, and $\sigma_D = (ne^2\tau/m)(1 - i\omega\tau)^{-1}$ is the Drude conductivity. From Eq. (20) one immediately can see that that the contribution to the DC current from the coupling to the cavity photon vanishes for any finite τ. This effect is similar to vanishing of the spin Hall current at any finite disorder [32–34]. We note that whereas the Hall conductivity vanishes at any finite disorder, the stationary current present in the absence of the external field is immune to disorder as shown in Sec. II.

IV. CONCLUSION

We have considered the generation of the chiral edge currents and spontaneous magnetization in the mesoscopic system comprising a laterally confined 2D electron gas placed inside a gyrotropic cavity. It has been shown that the diamagnetic and paramagnetic contributions to the edge current density have qualitatively different asymptotic behaviors when approaching the thermodynamics limit: whereas paramagnetic current density vanishes locally, the diamagnetic contribution approaches the finite value which results in the finite magnetization in the thermodynamic limit. We have also shown using semiclassical equations that the arbitrarily small disorder in 2DEG destroys the DC Hall conductivity, whereas leaving the AC Hall conductivity finite. These results suggest the cavity engineering of the material properties can serve as a powerful tool for controlling the transport properties in the mesoscopic systems.

ACKNOWLEDGMENTS

The main results of the paper were obtained with the support of Russian Science Foundation (Project No. 20-12-00224). I.V.T. acknowledges support by Grupos Consolidados UPV/EHU del Gobierno Vasco (Grant IT1453-22) and by the Spanish Ministerio de Ciencia e Innovacion (MICINN) (Project No. PID2020-112811GB-I00). I.V.I. And D.D.S acknowledge the support of "Basis" Foundation (Project No. 21-1-2-61-1).

APPENDIX A: FUNCTIONAL INTEGRAL FORMALISM

The expectation value of an arbitrary operator A, which in a general case depends on both fermionic and photonic operators, can be calculated as

$$\langle A(\psi^*, \psi, \mathbf{q})\rangle = \frac{1}{Z}\int D[\psi^*, \psi, \mathbf{q}]A(\psi^*, \psi)e^{S[\psi^*,\psi,\mathbf{q}]}, \tag{A1}$$

where Z is the partition function given by

$$Z = \int D[\psi^*, \psi, \mathbf{q}]e^{S[\psi^*,\psi,\mathbf{q}]}, \tag{A2}$$

$\int D[\psi^*, \psi, \mathbf{q}]$ denotes integration over all realizations of the fields; $S[\psi^*, \psi, \mathbf{q}]$ is the thermal action,

$$S[\psi^*, \psi, \mathbf{q}] = \int_0^\beta d\tau\left[\int d^2r\left\{\psi^*\left(-\partial_\tau - \frac{1}{2m}(\hat{\mathbf{p}} - \lambda\mathbf{q})^2\right)\psi\right\} - \frac{1}{2}\dot{\mathbf{q}}^2 - 2i\Delta[\dot{\mathbf{q}} \times \mathbf{q}] - \frac{\Omega_0^2}{2}\mathbf{q}^2\right], \tag{A3}$$

Let $S_0 = S|_{\lambda=0}$, then by expanding the exponent e^S near e^{S_0} in the powers of λ we can write an arbitrary expectation value in terms of the uncoupled fermionic and photonic Green's functions. Let us highlight that since S_0 is quadratic, only operators containing even powers of the fields can give a nonzero contribution after averaging, therefore, $Z = Z_0 + O(\lambda^2)$. For the same reason, expression $\int D[\psi^*, \psi, \mathbf{q}]\hat{j}_\mu e^{S[\psi^*,\psi,\mathbf{q}]}$ is, at least, proportional to λ^2. It means that one can take the zero-order partition function when calculating currents up to the second order of λ.

APPENDIX B: EXPLICIT EXPRESSIONS FOR CURRENTS

The explicit expression for the electron Green's function $G(\omega, n) = (i\omega + \mu - E_n)^{-1}$ and summation over fermionic Matsubara frequencies $\omega = \pi(2s+1)T,\ s \in \mathbb{Z}$, allows to rewrite (11) in the following way:

$$j^{\mathrm{d}}_{\mu}(\mathbf{r}) = \frac{\lambda^2}{m^2\beta}\sum_{\nu,\varepsilon}\sum_{n,n'}\frac{D_{\mu\nu}(\varepsilon)}{i\varepsilon + E_{n'} - E_n}[f(E'_n) - f(E_n)]\psi^*_{n'}(\mathbf{r})\psi_n(\mathbf{r})p^{nn'}_{\nu}, \tag{B1}$$

where $f(E_n)$ is the Fermi-Dirac distribution. Considering that an unperturbed system has time-reversal symmetry, and, therefore, both $\psi_n(\mathbf{r})$ and $\psi^*_n(\mathbf{r})$ are eigenfunctions corresponding to the same energy, we get

$$\begin{aligned} j^{\mathrm{d}}_{\mu}(\mathbf{r}) = {} & \frac{\lambda^2}{2m^2\beta}\sum_{\nu,\varepsilon}\sum_{n,n'}\frac{D_{\mu\nu}(\varepsilon)(E_{n'} - E_n)}{\varepsilon^2 + (E_{n'} - E_n)^2}[f(E'_n) - f(E_n)]\left[\psi^*_{n'}(\mathbf{r})\psi_n(\mathbf{r})p^{nn'}_{\nu} - \psi_{n'}(\mathbf{r})\psi^*_n(\mathbf{r})p^{n'n}_{\nu}\right] \\ & - \frac{\lambda^2}{2m^2\beta}\sum_{\nu,\varepsilon}\sum_{n,n'}\frac{i\varepsilon D_{\mu\nu}(\varepsilon)}{\varepsilon^2 + (E_{n'} - E_n)^2}[f(E'_n) - f(E_n)]\left[\psi^*_{n'}(\mathbf{r})\psi_n(\mathbf{r})p^{nn'}_{\nu} - \psi_{n'}(\mathbf{r})\psi^*_n(\mathbf{r})p^{n'n}_{\nu}\right], \end{aligned} \tag{B2}$$

where we used $\langle\psi^*_n|\hat{p}_\nu|\psi^*_{n'}\rangle = -\langle\psi_{n'}|\hat{p}_\nu|\psi_n\rangle$. The first line gives zero after summation over n, n' since the function under the sum is antisymmetric with respect to interchanging $n \leftrightarrow n'$. The second line has a nontrivial contribution only for the nondiagonal element of the photonic propagator, which follows directly from its time-reversal properties $D_{xx}(\varepsilon) = D_{yy}(\varepsilon),\ D_{yx}(\varepsilon) = -D_{yx}(-\varepsilon) = -D_{xy}(\varepsilon)$. Thus, the diamagnetic part of the current reads

$$j^{\mathrm{d}}_{\mu}(\mathbf{r}) = \frac{\lambda^2}{m^2\beta}\sum_{\varepsilon,n,n'}\frac{\varepsilon D_{\mu\nu}(\varepsilon)|_{\nu\neq\mu}}{\varepsilon^2 + (E_{n'} - E_n)^2}[f(E_{n'}) - f(E_n)]\mathrm{Im}\left[\psi^*_{n'}(\mathbf{r})\psi_n(\mathbf{r})p^{nn'}_{\nu}\right]. \tag{B3}$$

With analogous considerations one can obtain the following expression for the paramagnetic part of the current:

$$j^{\mathrm{p}}_{\mu}(\mathbf{r}) = \frac{\lambda^2}{\beta m^2}\sum_{\nu\neq\sigma,\varepsilon}\sum_{n,n',n_1}\frac{D_{\nu\sigma}(\varepsilon)\varepsilon}{E_n - E'_n}\left[\frac{f(E_n) - f(E_{n_1})}{(E_n - E_{n_1})^2 + \varepsilon^2} - \frac{f(E_{n'}) - f(E_{n_1})}{(E_{n'} - E_{n_1})^2 + \varepsilon^2}\right]\mathrm{Im}\left[p^{nn_1}_{\nu}p^{n_1n'}_{\sigma}j^{n'n}_{\mu}(\mathbf{r})\right]. \tag{B4}$$

If the variables can be separated, and the basis can be chosen as $\psi_n(\mathbf{r}) = \psi_{n_x}(x)\psi_{n_y}(y)$ with $n = (n_x, n_y)$ being a multi-index, the Eq. (B4) simplifies

$$j^{\mathrm{p}}_{y}(\mathbf{r}) = \frac{2\lambda^2}{\beta m^2}\sum_{\varepsilon}\sum_{(n_x,n_y),(n'_x,n'_y)}\frac{\varepsilon D_{yx}(\varepsilon)f(E_n)\left[E_{n_y} - E_{n'_y}\right]}{\left[\varepsilon^2 + \left(E_{n_x} - E_{n'_x}\right)^2\right]\left[\varepsilon^2 + \left(E_{n_y} - E_{n'_y}\right)^2\right]}\mathrm{Im}\left[p^{n_yn'_y}_{y}p^{n_xn'_x}_{x}j^{n'n}_{y}(\mathbf{r})\right], \tag{B5}$$

where $E_{n_{x(y)}}$'s are eigenenergies of the Hamiltonian projected on the subspace corresponding to coordinate $x(y)$, and $p^{n_{x,y}n'_{x,y}}_{x,y} = \langle\psi_{n_{x,y}}|\hat{p}_{x,y}|\psi_{n'_{x,y}}\rangle$.

APPENDIX C: CALCULATION OF EDGE CURRENT FOR THE SEMI-INFINITE 2DEG

Eigenfunctions of the semi-infinite 2DEG which occupies half-plane $x > 0$ can be parametrized by the wave vector, and they are given as $\psi_{\mathbf{k}} = \sqrt{2/\pi}\sin(k_x x)e^{ik_y y}$. From Eq. (B1) we can see that the diagonal element of the photonic Green's function does not have any contribution to the current since $\langle\mathbf{k}|\hat{p}_y|\mathbf{k}'\rangle = \delta(\mathbf{k} - \mathbf{k})k_y$, and the δ function leads to the trivial result. $\langle k_x|\hat{p}_x|k'_x\rangle = -i\langle k_x|\partial_x U|k'_x\rangle/(E_{\mathbf{k}'} - E_{\mathbf{k}})$, and using the parity of the photonic Green's function, we obtain

$$j^{\mathrm{d}}_{y}(\mathbf{r}) = \sum_{\mathbf{k},\mathbf{k}'}\delta(k_y - k'_y)\sum_{\varepsilon}\frac{\varepsilon D_{yx}(\varepsilon)\langle k'_x|\partial_x U|k_x\rangle}{\varepsilon^2 + (E_{\mathbf{k}'} - E_{\mathbf{k}})^2}\frac{f_{\mathbf{k}'} - f_{\mathbf{k}}}{E_{\mathbf{k}'} - E_{\mathbf{k}}}\psi_{k'_x}(x)\psi^*_{k_x}(x). \tag{C1}$$

Now we want to calculate the integral edge current created $J_{\mathrm{edge}} = \int_0^\infty dx\, j^{\mathrm{d}}_y(x)$. Integration over x results in $\delta(k_x - k'_x)$, and, therefore, we have

$$J_{\mathrm{edge}} = \sum_{\mathbf{k},\varepsilon}\frac{\varepsilon D_{yx}(\varepsilon)}{\varepsilon^2 + (E_{\mathbf{k}'} - E_{\mathbf{k}})^2}\langle k_x|\partial_x U|k_x\rangle\left.\frac{\partial f}{\partial E}\right|_{E=E_{\mathbf{k}}}. \tag{C2}$$

Observing now that $\langle k_x|\partial_x U|k_x\rangle = 2k_x^2/m = 2k_x\partial E_{\mathbf{k}}/\partial k_x$, we can perform summation over $\mathbf{k}$ and arrive at

$$J_{\mathrm{edge}} = -\frac{\lambda^2 n_0}{m^2}\sum_{\varepsilon}\frac{D_{yx}(\varepsilon)}{\varepsilon}, \tag{C3}$$

where n_0 is the density of electrons in the bulk. Summation over ε results in the expression (13). We can see that this result coincides with the universal result from Eq. (9) in the main text.

The paramagnetic contribution is locally zero. This can be immediately seen from Eq. (B5) in the clean limit the momentum matrix element for the momentum along the translationally invariant direction is just a δ function, and this leads to vanishing of the term $E_{n_y} - E_{n'_y}$ in the numerator.

APPENDIX D: DIAMAGNETIC CONTRIBUTION TO THE MAGNETIC MOMENT FOR A HARMONIC CONFINEMENT

In the case of a harmonic confinement with $U(\mathbf{r}) = \frac{1}{2}m\omega^2\mathbf{r}^2$ the diamagnetic part of the magnetic moment can be calculated exactly using the sum rule Eq. (8). Starting from the general expression Eq. (4) for the diamagnetic current in terms of the density-current response function we represent the magnetic moment as follows:

$$m_z^{\mathrm{d}} = \frac{1}{2}\epsilon_{z\mu\nu}\int d\mathbf{r}\, r_\mu j_\nu^d(\mathbf{r}) = \frac{1}{2}\epsilon_{z\mu\nu}\frac{\lambda^2}{m\beta}\sum_\varepsilon D_{\nu\alpha}(\varepsilon)\int d\mathbf{r}\, d\mathbf{r}'\, r_\nu \chi_{n,j_\alpha}(\mathbf{r},\mathbf{r}',\varepsilon). \tag{D1}$$

Inserting here the identity Eq. (8) and performing the partial integration in the first term containing ∇n we get

$$m_z^{\mathrm{d}} = \frac{1}{2}\epsilon_{z\mu\nu}\frac{\lambda^2}{m\beta}\sum_\varepsilon \frac{D_{\nu\alpha}(\varepsilon)}{m\varepsilon}\left[N\delta_{\mu\alpha} + m\omega^2\int d\mathbf{r}\, d\mathbf{r}' r_\nu \chi_{n,n}(\mathbf{r},\mathbf{r}',\varepsilon) r_\alpha\right]. \tag{D2}$$

The second therm in the square brackets is readily found from the linear-response version of the harmonic potential theorem [30],

$$\int d\mathbf{r}\, d\mathbf{r}' r_\nu \chi_{n,n}(\mathbf{r},\mathbf{r}',\varepsilon) r_\alpha = -\frac{N}{m(\varepsilon^2+\omega^2)}. \tag{D3}$$

By inserting this identity into the previous equation we arrive at the following final result,

$$m_z^{\mathrm{d}} = \frac{\lambda^2 N}{m^2\beta}\sum_\varepsilon \frac{\varepsilon D_{yx}(\varepsilon)}{\varepsilon^2+\omega^2}, \tag{D4}$$

which, in the limit $\omega \to 0$ reduces to the universal limiting form of the magnetization Eq. (10).

APPENDIX E: SUMMATION OVER BOSONIC MATSUBARA FREQUENCIES FOR THE PARABOLIC CONFINING POTENTIAL

We have shown that currents and magnetization for the parabolic potential are proportional to the following summation over Matsubara frequencies that can be calculated explicitly,

$$\frac{1}{\beta}\sum_\varepsilon \frac{\varepsilon D_{yx}(\varepsilon)}{\varepsilon^2+\omega^2} = \frac{\Delta}{2}\left[\frac{\Omega_+[1+2n_{\mathrm{B}}(\Omega_+)]}{(\Omega_+^2-\Omega_-^2)(\omega^2-\Omega_+^2)} - \frac{\Omega_-[1+2n_{\mathrm{B}}(\Omega_-)]}{(\Omega_+^2-\Omega_-^2)(\omega^2-\Omega_-^2)} - \frac{\omega[1+2n_{\mathrm{B}}(\omega)]}{(\Omega_+^2-\omega^2)(\Omega_-^2-\omega^2)}\right], \tag{E1}$$

$$\begin{aligned}\frac{1}{\beta}\sum_\varepsilon \frac{\varepsilon D_{yx}(\varepsilon)}{(\varepsilon^2+\omega^2)^2} = \frac{\Delta}{2}\Bigg[&-\frac{[1+2n_{\mathrm{B}}(\omega)+\omega\partial_\omega n_{\mathrm{B}}(\omega)]}{2\omega(\omega^2-\Omega_-^2)(\omega^2-\Omega_+^2)} + \frac{(\Omega_-^2\Omega_+^2-\omega^4)[1+2n_B(\Omega)]}{\omega(\omega^2-\Omega_-^2)^2(\Omega^2-\Omega_+^2)^2}\\ &+\frac{\Omega_-[1+2n_{\mathrm{B}}(\Omega_-)]}{(\omega^2-\Omega_-^2)^2(\Omega_-^2-\Omega_+^2)} - \frac{\Omega_+[1+2n_{\mathrm{B}}(\Omega_+)]}{(\omega^2-\Omega_+^2)^2(\Omega_-^2-\Omega_+^2)}\Bigg].\end{aligned} \tag{E2}$$

[1] A. A. Anappara, S. De Liberato, A. Tredicucci, C. Ciuti, G. Biasiol, L. Sorba, and F. Beltram, Signatures of the ultrastrong light-matter coupling regime, Phys. Rev. B **79**, 201303(R) (2009).

[2] R. Chikkaraddy, B. De Nijs, F. Benz, S. J. Barrow, O. A. Scherman, E. Rosta, A. Demetriadou, P. Fox, O. Hess, and J. J. Baumberg, Single-molecule strong coupling at room temperature in plasmonic nanocavities, Nature (London) **535**, 127 (2016).

[3] A. F. Kockum, A. Miranowicz, S. De Liberato, S. Savasta, and F. Nori, Ultrastrong coupling between light and matter, Nat. Rev. Phys. **1**, 19 (2019).

[4] H. Hübener, U. De Giovannini, C. Schäfer, J. Andberger, M. Ruggenthaler, J. Faist, and A. Rubio, Engineering quantum materials with chiral optical cavities, Nature Mater. **20**, 438 (2021).

[5] F. Schlawin, D. M. Kennes, and M. A. Sentef, Cavity quantum materials, Appl. Phys. Rev. **9**, 011312 (2022).

[6] J. Li, L. Schamriß, and M. Eckstein, Effective theory of lattice electrons strongly coupled to quantum electromagnetic fields, Phys. Rev. B **105**, 165121 (2022).

[7] A. Thomas, E. Devaux, K. Nagarajan, T. Chervy, M. Seidel, D. Hagenmüller, S. Schütz, J. Schachenmayer, C. Genet, G. Pupillo *et al.*, Exploring superconductivity under strong coupling with the vacuum electromagnetic field, arXiv:1911.01459.

[8] J. B. Curtis, Z. M. Raines, A. A. Allocca, M. Hafezi, and V. M. Galitski, Cavity Quantum Eliashberg Enhancement of Superconductivity, Phys. Rev. Lett. **122**, 167002 (2019).

[9] M. A. Sentef, M. Ruggenthaler, and A. Rubio, Cavity quantum-electrodynamical polaritonically enhanced electron-phonon

coupling and its influence on superconductivity, Sci. Adv. **4**, eaau6969 (2018).
[10] F. Schlawin, A. Cavalleri, and D. Jaksch, Cavity-Mediated Electron-Photon Superconductivity, Phys. Rev. Lett. **122**, 133602 (2019).
[11] J. Li and M. Eckstein, Manipulating Intertwined Orders in Solids with Quantum Light, Phys. Rev. Lett. **125**, 217402 (2020).
[12] Y. Ashida, A. İmamoğlu, J. Faist, D. Jaksch, A. Cavalleri, and E. Demler, Quantum Electrodynamic Control of Matter: Cavity-Enhanced Ferroelectric Phase Transition, Phys. Rev. X **10**, 041027 (2020).
[13] D. Guerci, P. Simon, and C. Mora, Superradiant Phase Transition in Electronic Systems and Emergent Topological Phases, Phys. Rev. Lett. **125**, 257604 (2020).
[14] X. Wang, E. Ronca, and M. A. Sentef, Cavity quantum electrodynamical chern insulator: Towards light-induced quantized anomalous hall effect in graphene, Phys. Rev. B **99**, 235156 (2019).
[15] F. Herrera and F. C. Spano, Cavity-Controlled Chemistry in Molecular Ensembles, Phys. Rev. Lett. **116**, 238301 (2016).
[16] T. W. Ebbesen, Hybrid light–matter states in a molecular and material science perspective, Acc. Chem. Res. **49**, 2403 (2016).
[17] K. Bennett, M. Kowalewski, and S. Mukamel, Novel photochemistry of molecular polaritons in optical cavities, Faraday Discuss. **194**, 259 (2016).
[18] L. A. Martínez-Martínez, R. F. Ribeiro, J. Campos-González-Angulo, and J. Yuen-Zhou, Can ultrastrong coupling change ground-state chemical reactions? ACS Photonics **5**, 167 (2018).
[19] I. V. Tokatly, Time-Dependent Density Functional Theory for Many-Electron Systems Interacting with Cavity Photons, Phys. Rev. Lett. **110**, 233001 (2013).
[20] M. Ruggenthaler, J. Flick, C. Pellegrini, H. Appel, I. V. Tokatly, and A. Rubio, Quantum-electrodynamical density-functional theory: Bridging quantum optics and electronic-structure theory, Phys. Rev. A **90**, 012508 (2014).
[21] C. Schäfer, M. Ruggenthaler, and A. Rubio, Ab initio nonrelativistic quantum electrodynamics: Bridging quantum chemistry and quantum optics from weak to strong coupling, Phys. Rev. A **98**, 043801 (2018).
[22] G. M. Andolina, F. M. D. Pellegrino, V. Giovannetti, A. H. MacDonald, and M. Polini, Cavity quantum electrodynamics of strongly correlated electron systems: A no-go theorem for photon condensation, Phys. Rev. B **100**, 121109(R) (2019).
[23] P. Nataf and C. Ciuti, No-go theorem for superradiant quantum phase transitions in cavity qed and counter-example in circuit qed, Nat. Commun. **1**, 72 (2010).
[24] G. M. Andolina, F. M. D. Pellegrino, A. Mercurio, O. Di Stefano, M. Polini, and S. Savasta, A non-perturbative no-go theorem for photon condensation in approximate models, arXiv:2104.09468.
[25] V. Rokaj, M. Ruggenthaler, F. G. Eich, and A. Rubio, Free electron gas in cavity quantum electrodynamics, Phys. Rev. Res. **4**, 013012 (2022).
[26] P. Pilar, D. De Bernardis, and P. Rabl, Thermodynamics of ultrastrongly coupled light-matter systems, Quantum **4**, 335 (2020).
[27] D. Braak, Integrability of the Rabi Model, Phys. Rev. Lett. **107**, 100401 (2011).
[28] M.-J. Hwang, R. Puebla, and M. B. Plenio, Quantum Phase Transition and Universal Dynamics in the Rabi Model, Phys. Rev. Lett. **115**, 180404 (2015).
[29] I. V. Tokatly, D. R. Gulevich, and I. Iorsh, Vacuum anomalous hall effect in gyrotropic cavity, Phys. Rev. B **104**, L081408 (2021).
[30] G. Vignale, Sum rule for the linear density response of a driven electronic system, Phys. Lett. A **209**, 206 (1995).
[31] M. V. Durnev and S. A. Tarasenko, Rectification of ac electric current at the edge of 2d electron gas, Phys. Status Solidi B **258**, 2000291 (2021).
[32] E. G. Mishchenko, A. V. Shytov, and B. I. Halperin, Spin Current and Polarization in Impure Two-Dimensional Electron Systems with Spin-Orbit Coupling, Phys. Rev. Lett. **93**, 226602 (2004).
[33] O. V. Dimitrova, Spin-hall conductivity in a two-dimensional rashba electron gas, Phys. Rev. B **71**, 245327 (2005).
[34] R. Raimondi and P. Schwab, Spin-hall effect in a disordered two-dimensional electron system, Phys. Rev. B **71**, 033311 (2005).